AGU PUBLICATIONS

Paleoceanography

RESEARCH ARTICLE
10.1002/2014PA002667

**Key Points:**
- AMOC still active during Heinrich Stadial 1 but weaker than during the LGM
- Weaker AMOC caused reduced NADW volume and NADW $\delta^{13}C$ source decrease
- Amplitude of early deglacial $\delta^{13}C$ decrease correlated to glacial NADW fraction

**Supporting Information:**
- Tables S1–S7
- Figures S1–S4

**Correspondence to:**
D. W. Oppo,
doppo@whoi.edu

**Citation:**
Oppo, D. W., W. B. Curry, and J. F. McManus (2015), What do benthic $\delta^{13}C$ and $\delta^{18}O$ data tell us about Atlantic circulation during Heinrich Stadial 1?, *Paleoceanography*, *30*, 353–368, doi:10.1002/2014PA002667.

Received 6 MAY 2014
Accepted 6 MAR 2015
Accepted article online 14 MAR 2015
Published online 13 APR 2015



# What do benthic $\delta^{13}C$ and $\delta^{18}O$ data tell us about Atlantic circulation during Heinrich Stadial 1?

**Delia W. Oppo[1], William B. Curry[2], and Jerry F. McManus[3]**

[1]Department of Geology and Geophysics, Woods Hole Oceanographic Institution, Woods Hole, Massachusetts, USA, [2]Bermuda Institute of Ocean Sciences, St. George's, Bermuda, [3]Lamont-Doherty Earth Observatory, Columbia University, Palisades, New York, USA

**Abstract** Approximately synchronous with the onset of Heinrich Stadial 1 (HS1), $\delta^{13}C$ decreased throughout most of the upper (~1000–2500 m) Atlantic, and at some deeper North Atlantic sites. This early deglacial $\delta^{13}C$ decrease has been alternatively attributed to a reduced fraction of high-$\delta^{13}C$ North Atlantic Deep Water (NADW) or to a decrease in the NADW $\delta^{13}C$ source value. Here we present new benthic $\delta^{18}O$ and $\delta^{13}C$ records from three relatively shallow (~1450–1650 m) subpolar Northeast Atlantic cores. With published data from other cores, these data form a depth transect (~1200–3900 m) in the subpolar Northeast Atlantic. We compare Last Glacial Maximum (LGM) and HS1 data from this transect with data from a depth transect of cores from the Brazil Margin. The largest LGM-to-HS1 decreases in both benthic $\delta^{13}C$ and $\delta^{18}O$ occurred in upper waters containing the highest NADW fraction during the LGM. We show that the $\delta^{13}C$ decrease can be explained entirely by a lower NADW $\delta^{13}C$ source value, entirely by a decrease in the proportion of NADW relative to Southern Ocean Water, or by a combination of these mechanisms. However, building on insights from model simulations, we hypothesize that reduced ventilation due to a weakened but still active Atlantic Meridional Overturning Circulation also contributed to the low $\delta^{13}C$ values in the upper North Atlantic. We suggest that the benthic $\delta^{18}O$ gradients above ~2300 m at both core transects indicate the depth to which heat and North Atlantic deglacial freshwater had mixed into the subsurface ocean by early HS1.

## 1. Introduction

It is generally inferred that the Atlantic Meridional Overturning Circulation (AMOC) was weaker during two deglacial North Atlantic cold events, Heinrich Stadial 1 (HS1) and the Younger Dryas (YD) [e.g., *Boyle and Keigwin*, 1987; *McManus et al*., 2004, among many others]. Hypotheses of the ocean's role in influencing deglacial surface climate and atmospheric $CO_2$ concentration rely on a thorough understanding of past deep ocean circulation [e.g., *Sigman et al*., 2008, 2010; *Toggweiler et al*., 2006; *Meckler et al*., 2013; *Kwon et al*., 2012; *Adkins*, 2013; *Yu et al*., 2014; *Schmittner and Lund*, 2015; among many others], yet recent studies suggest significant gaps in our understanding of deglacial Atlantic circulation changes. For example, and as we discuss in greater detail in section 2.4, most explanations for an early deglacial $\delta^{13}C$ decrease that occurred throughout much of the Atlantic Ocean above 2500 m, and in the deep North Atlantic, suggest that it was a response to the hypothesized AMOC reduction, but the precise mechanisms invoked differ. Some investigators conclude that the fraction of North Atlantic Deep Water (NADW) in the upper (and deep) North Atlantic decreased during these events, perhaps in association with shoaling of the transition zone between NADW and deep Southern Ocean Water (SOW) [*Curry et al*., 1999; *Oppo and Curry*, 2012; *Xie et al*., 2012; *Meckler et al*., 2013], lowering $\delta^{13}C$. Others suggest that NADW continued to flow southward between ~1000–2200 m but that it had lower $\delta^{13}C$ (and $\delta^{18}O$) values during HS1 than during the Last Glacial Maximum (LGM) [e.g., *Waelbroeck et al*., 2011; *Lund et al*., 2015].

Here we present new data from the subpolar North Atlantic, from cores taken from ~1450 to 1630 m depth on the east side of the Reykjanes Ridge, and having relatively high early deglacial accumulation rates (~9–15 cm/kyr) compared to other supbolar North Atlantic cores from similar depths (~5 cm/kyr), as described in section 3. Together with published records, our new records form a subpolar North Atlantic depth transect that extends from ~1200 to 3900 m. We compare benthic $\delta^{18}O$ and $\delta^{13}C$ LGM and HS1 data from this transect to data from a depth transect of cores from the Brazil Margin. We show that either a large decrease in the NADW $\delta^{13}C$ source value or a large reduction in the influence of NADW relative to southern sources can explain the early deglacial $\delta^{13}C$ decrease; we then argue that a weaker AMOC caused the $\delta^{13}C$ decrease by a

combination of these mechanisms but that accumulation of respired carbon likely also contributed to the low $\delta^{13}C$ values in the upper North Atlantic.

## 2. Background

### 2.1. $\delta^{13}C$ and $\delta^{18}O$ as Water Mass Tracers

When primary producers take up nutrients and carbon, they preferentially remove $^{12}C$, leaving surface waters enriched in $^{13}C$. Organic matter remineralization adds nutrients, and carbon with low $^{13}C/^{12}C$, to deepwater. As a result of these processes, nutrients and $\delta^{13}C$ of dissolved inorganic carbon (here $\delta^{13}C$) are generally negatively correlated, and water masses that contain a relatively high fraction of surface water, like NADW, are nutrient depleted and have high $\delta^{13}C$ values; nutrient-rich waters like Antarctic Bottom Water (AABW) have relatively low $\delta^{13}C$ values [*Kroopnick*, 1985]. The $\delta^{13}C$ in surface water is also influenced by air-sea gas exchange, which is favored in cold, windy regions [*Mook et al*., 1974; *Liss and Merlivat*, 1986; *Broecker and Maier-Reimer*, 1992]. Within the ocean interior, $\delta^{13}C$ of a water mass may change due to mixing with waters having different $\delta^{13}C$ values, and/or due to the oxidation of low-$\delta^{13}C$ organic matter [*Kroopnick*, 1985]. Within the deep western Atlantic, where the residence time of deep water is relatively short (several hundred years, away from the western boundary) [e.g., *Stuiver et al*., 1983], the $\delta^{13}C$ distribution largely reflects mixing between NADW and AABW [e.g., *Oppo and Fairbanks*, 1987; *Curry et al*., 1988].

Among genera of benthic foraminifera, *Cibicidoides* seem to record the $\delta^{13}C$ of dissolved inorganic carbon most reliably [*Duplessy et al*., 1984; *Belanger et al*., 1981; *Graham et al*., 1981], except in regions of very high productivity [*Mackensen et al*., 1993]. *Cibicidoides* $\delta^{13}C$ is commonly used to map the past sea water distribution of $\delta^{13}C$, which is then used to infer the distribution of deep water masses and their geographic and bathymetric distributions. As for any property, deciphering water mass distributions based on nutrient proxies requires making assumptions about or knowledge of source water ("end-member") values [e.g., *Mix and Fairbanks*, 1985; *Oppo and Fairbanks*, 1987; *LeGrand and Wunsch*, 1995; *Wunsch*, 2003; *Curry and Oppo*, 2005].

The $\delta^{18}O$ of benthic foraminifera ($\delta^{18}O_{BF}$) is also potentially a valuable deepwater tracer. Foraminiferal $\delta^{18}O$ is a function of both calcification temperature and the $\delta^{18}O$ of seawater ($\delta^{18}Osw$) [e.g., *Erez and Luz*, 1983; *Bemis et al*., 1998]. Surface $\delta^{18}Osw$ is largely controlled by the hydrologic cycle and is generally positively correlated to salinity [*Craig and Gordon*, 1965], and, as a result, with water density [*Lynch-Stieglitz et al*., 1999; *Lynch-Stieglitz*, 2001]. However, $\delta^{18}Osw$ and salinity may be decoupled during brine formation [*Craig and Gordon*, 1965]. Water masses that include a significant proportion of brines have lower $\delta^{18}Osw$ for their salinity (and density). $\delta^{18}O_{BF}$ values reflect conservative sea water properties and, assuming negligible geothermal and pressure heating effects, $\delta^{18}O_{BF}$ in the ocean interior can only change due to mixing between water masses.

### 2.2. Modern Atlantic Water Mass Distribution

Today, NADW flows southward centered at ~2.5–3 km water depth. AABW flows northward below NADW and can be traced by its low salinity as far north as 40°N. Upper Circumpolar Deep Water and Antarctic Intermediate Water (AAIW) flow northward above NADW, with AAIW reaching as far north as ~20°N. This deepwater geometry is reflected in the $\delta^{13}C$ of $\Sigma CO_2$, with NADW having higher values than the underlying and overlying Southern Ocean Water masses [*Kroopnick*, 1985]. NADW is also saltier and has a lower phosphate concentration than the Southern Ocean Water masses [*Bainbridge*, 1981].

### 2.3. LGM Western Atlantic Water Mass Distribution

Reconstructions of the glacial distributions of the $\delta^{13}C$ and dissolved cadmium (Cd) in the deep Atlantic Ocean suggest that NADW, today filling most of the deep North Atlantic, shoaled to $<2$ km (often called Glacial North Atlantic Intermediate Water following *Boyle and Keigwin* [1987], here NADW), and Southern Ocean Water (SOW) filled the deep Atlantic below 2 km even as far north as the subpolar North Atlantic [e.g., *Boyle and Keigwin*, 1987; *Oppo and Fairbanks*, 1987; *Duplessey et al*., 1988; *Curry et al*., 1988; *Oppo and Lehman*, 1993; *Curry and Oppo*, 2005; *Marchitto and Broecker*, 2006]. Paired planktonic and benthic foraminifera radiocarbon [e.g., *Skinner and Shackleton*, 2004; *Keigwin*, 2004], paired coral radiocarbon and U-series dates [*Robinson et al*., 2005], neodymium isotope data [*Roberts et al*., 2010], foraminifera Zn/Ca [*Marchitto et al*., 2002], and carbonate proxy data [*Yu et al*., 2010] also suggest the presence of SOW in the deep glacial North Atlantic. Benthic $\delta^{13}C$,

$\delta^{18}O$, and Cd/Ca data clearly identify the depth range (1000–1200 m, adjusted for sea level change) of low-$\delta^{13}C$, high-Cd AAIW at ~27°S in the glacial western South Atlantic [*Curry and Oppo*, 2005; *Makou et al*., 2010].

A recent glacial water mass decomposition using benthic Cd/Ca, $\delta^{13}C$, and $\delta^{18}O$ data suggests that while the core of glacial NADW was approximately 1000 m shallower than today [*Gebbie*, 2014], consistent with previous inferences, the boundary between water masses, as defined by equal proportions of upper northern and deeper southern waters, may have been at roughly the same depth as today. Importantly, in this decomposition, a seemingly small change in water mass flow paths in the South Atlantic results in enhanced advection of remineralized organic matter from the middepth Southern Ocean to the deep North Atlantic, and thus more nutrients and lower $\delta^{13}C$ values in the deep North Atlantic. By attributing some decrease in $\delta^{13}C$ at depth to remineralized organic matter, the contribution of SOW to the deep glacial Atlantic is less than previously deduced by assuming conservative behavior of $\delta^{13}C$. These results demonstrate that even subtle oceanographic changes may decouple $\delta^{13}C$ from water mass composition. Similarly, results in *Kwon et al*. [2012] suggest that changes in the relative proportions of preformed and regenerated nutrients that may accompany circulation changes can significantly reduce the utility of $\delta^{13}C$ as a water mass tracer.

### 2.4. Water Mass Distribution in the Deglacial Western Atlantic

The prevailing paradigm of a weaker Atlantic Meridional Overturning Circulation (AMOC) during North Atlantic deglacial cold events, Heinrich Stadial 1 (HS1) and the Younger Dryas (YD), was also originally based on nutrient proxy records from the deep Atlantic [*Boyle and Keigwin*, 1987; *Keigwin and Lehman*, 1994; *Vidal et al*., 1998]. Although not without potential limitations [e.g., *Chase et al*., 2002; *Keigwin and Boyle*, 2008], deep North Atlantic $^{231}Pa/^{230}Th$ records are consistent with this view [e.g., *McManus et al*., 2004; *Gherardi et al*., 2009; *Burke et al*., 2011; *Bradtmiller et al*., 2014], as are sedimentary grain size records [e.g., *Praetorius et al*., 2008] and evidence of warming of the western Atlantic deep thermocline [e.g., *Rühlemann et al*., 2004; *Came et al*., 2007; *Schmidt et al*., 2012; *Lynch-Stieglitz et al*., 2014].

Low $\delta^{13}C$, high Cd/Ca, and low radiocarbon values during North Atlantic cold events suggest a decreased presence of NADW relative to SOW in the deep North Atlantic [e.g., *Boyle and Keigwin*, 1987; *Keigwin and Lehman*, 1994; *Robinson et al*., 2005; *Skinner and Shackleton*, 2004]. Low $\delta^{13}C$ values early in the deglaciation have also been documented between ~1600 and 2500 m in the southwestern Atlantic [*Tessin and Lund*, 2013], between 1200 and 2300 m in the North Atlantic [e.g., *Vidal et al*., 1997; *Thornalley et al*., 2010; *Curry et al*., 1999; *Rickaby and Elderfield*, 2005; among many others], and above 1800 m in the tropical Atlantic [e.g., *Oppo and Fairbanks*, 1987; *Zahn and Stuber*, 2002; *Lynch-Stieglitz et al*., 2014]. While a few studies suggested that greater northward advection of AAIW during HS1 caused low $\delta^{13}C$ at relatively shallow depths [e.g., *Rickaby and Elderfield*, 2005; *Pahnke et al*., 2008], more recent studies using cores from modern AAIW depths suggest that the northward extent of AAIW decreased during HS1 and the YD, presumably in response to a reduced AMOC [e.g., *Came et al*., 2008; *Xie et al*., 2012; *Huang et al*., 2014]. As already noted in section 1, low HS1 $\delta^{13}C$ values have often been attributed to the effects of reduced AMOC—to the effect of AMOC on the fraction of NADW at depth [e.g., *Keigwin and Lehman*, 1994], on the depth of the NADW/SOW water mass boundary [e.g., *Curry et al*., 1999; *Oppo and Curry*, 2012], and on the NADW source value [*Lund et al*., 2015]. Lower $\delta^{13}C$ (and $\delta^{18}O_{BF}$) NADW source values have also been attributed to the incorporation into NADW of brines formed in the Nordic Sea [*Dokken and Jansen*, 1999, *Waelbroeck et al*., 2006; *Meland et al*., 2008; *Thornalley et al*., 2010], where $\delta^{13}C$ may have been low due to reduced air-sea gas exchange [*Waelbroeck et al*., 2011].

Thus, although there is agreement that the early deglacial $\delta^{13}C$ decrease is in some way associated with Atlantic circulation change, there is still not a consensus on how the middepth (~1600–2500 m) Atlantic was ventilated, or on the precise mechanism(s) causing the early deglacial (HS1) $\delta^{13}C$ decrease.

## 3. Isotope Data and Age Models

To better constrain glacial and deglacial northern source values, we present new benthic (mostly *C. wuellerstorfi*) isotope data from three cores (EW9302-24GGC, EW9302-25GGC, and EW9302-26GGC) collected on the east side of the Reykjanes Ridge, south of Iceland, between 1450 and 1630 m (Table 1 and Figure S1 in the supporting information). Age models are based on radiocarbon dates (supporting information Table S1) converted to calendar ages using the Marine13 calibration curve [*Reimer et al*., 2013] and deglacial reservoir ages for the

**Table 1.** Core Locations

| Core | Latitude | Longitude | Depth (m) | Data | Age Model |
|---|---|---|---|---|---|
| KNR159-5-36GGC | −27.27 | −46.47 | 1268 | a,b | c |
| KNR159-5-17JPC | −27.70 | −46.48 | 1627 | b,d | c |
| KNR159-5-78GGC | −27.48 | −46.33 | 1820 | b | c |
| KNR159-5-33GGC | −27.57 | −46.18 | 2082 | b | c |
| KNR159-5-42JPC | −27.76 | −46.63 | 2296 | b,d | c |
| KNR159-5-73GGC | −27.89 | −46.04 | 2397 | b | e |
| KNR159-5-30GGC | −28.13 | −46.06 | 2500 | f | c |
| KNR159-5-125GGC | −29.52 | −45.75 | 3589 | f | c |
| KNR159-5-22GGGC | −29.79 | −43.59 | 3924 | f | c |
| RAPiD-10-1P | 62.98 | −17.59 | 1237 | g | c |
| EW9302-26GGC | 62.32 | −21.46 | 1450 | e | e |
| EW9302-25GGC | 62.06 | −21.47 | 1523 | e | e |
| NEAP4k | 61.29 | −24.17 | 1627 | h | c,e |
| EW9302-24GGC | 61.76 | −21.67 | 1629 | e | e |
| ODP 984 | 61.00 | −24.00 | 1648 | i | c,e |
| RAPiD-15-4P | 63.29 | −17.13 | 2133 | g | e |
| RAPiD-17-5P | 61.48 | −19.54 | 2303 | g | e |
| KN166-14-JPC-13 | 53.06 | −33.53 | 3082 | j | j |
| IODP U1308 | 49.88 | −24.24 | 3883 | k | e |

[a] *Came et al.* [2003].
[b] *Tessin and Lund* [2013].
[c] *Lund et al.* [2015].
[d] *Curry and Oppo* [2005].
[e] This study.
[f] *Hoffman and Lund* [2012].
[g] *Thornalley et al.* [2010].
[h] *Rickaby and Elderfield* [2005].
[i] *Praetorius et al.* [2008].
[j] *Hodell et al.* [2010].
[k] *Hodell et al.* [2008].

North Atlantic from *Stern and Lisiecki* [2013]. Implied LGM accumulation rates range from 25 to 30 cm/kyr. Implied early deglacial accumulation rates are ~15 cm/kyr for EW9302-24GGC and EW9302-26GGC, and ~9 cm/kyr for EW9302-25GGC.

EW9302 benthic isotope data (supporting information Table S2) are used in conjunction with published benthic $\delta^{18}O$ and $\delta^{13}C$ data from North and South Atlantic cores deeper than ~1200 m. All the South Atlantic data come from Brazil Margin cores we collected along a depth transect (27°S–30°S; 43°W–47°W) (Figure S1) and were generated in two laboratories (Woods Hole Oceanographic Institution (WHOI) and University of Michigan). To minimize differences due to latitude, we only include North Atlantic data from cores collected north of 49°N. However, the cores span a wide geographic range (~50°N–65°N, 15°W–34°W), and data were collected in several laboratories, including WHOI (EW9302 cores, Ocean Drilling Project site 984; here "ODP 984"). For simplicity, we refer to the modern water depths of cores in our discussions, rather than their LGM or HS1 water depth.

For most Brazil Margin cores, we use age models based on radiocarbon data converted to calendar age from *Lund et al*. [2015]. Many Brazil Margin cores show radiocarbon reversals in their deglacial sections, and we follow previous work on which radiocarbon and isotope data to include [*Hoffman and Lund*, 2012; *Tessin and Lund*, 2013; *Lund et al*., 2015]. Implied LGM and early deglacial accumulation rates are typically high, ranging from 15 to 35 cm/kyr. A few cores (KNR159-5-30GGC, KNR159-42JPC, and KNR159-125GGC) have lower LGM and deglacial accumulation rates (5–10 cm/kyr). We also include data from Brazil Margin core KNR159-5-73JPC (2397 m) (supporting information Table S3), whose age model is based on two radiocarbon dates and correlating features of the $\delta^{18}O_{BF}$ to the better dated record from KNR159-5-42JPC, only 100 m shallower, as described in the supplementary information (Figure S2). Implied LGM (~5 cm/kyr) and deglacial (~9/cm/kyr) accumulation rates for this core are modest.

For the three RAPiD subpolar North Atlantic cores, we make small age adjustments, as the published age models [*Thornalley et al*., 2010] result in an HS1 that is younger than the interval we use here. For core RAPiD-10-1P, we

use the age model of *Lund et al.* [2015], who tied the onset of the early HS1 $\delta^{13}C$ decrease in RAPiD-10-1P to that of a core from the western tropical Atlantic (M35003, 12° 50′N, 61° 15′W ~1299 m [*Zahn and Stuber*, 2002]). This approach results in a timing of the early deglacial $\delta^{13}C$ decrease similar to the nearby EW9302 cores, whose age models are based on radiocarbon ages and independent of the assumption that the subpolar North Atlantic $\delta^{13}C$ decreased approximately synchronously with the $\delta^{13}C$ decrease in the low-latitude western Atlantic; we thus retain this age model. We tie the initial benthic $\delta^{13}C$ decreases in RAPiD-17-5P and RAPiD-15-4P to those of the other North Atlantic records (supporting information Table S4). Our age models imply LGM and early deglacial accumulation rates of ~30 cm/kyr and 8 cm/kyr in RAPiD-10-1P and RAPiD-15-4P, respectively. For RAPiD-17-5P, implied accumulation rates are ~15 cm/kyr for the LGM and ~3–7 cm/kyr for the early deglaciation. We also use a new age model for ODP 984 [*Praetorius et al.*, 2008] based on radiocarbon ages with variable reservoir age [*Lund et al.*, 2015] and an additional constraint based we provided on the relative abundances of the polar planktonic foraminifera *Neogloboquadrina pachyderma* (left coiling), which allows identification of the peak of the Bølling-Allerød warm period (Table S5 and Figure S3 in the supporting information). This age model implies accumulation rates of ~30 cm/kyr for the LGM and ~4 cm/kyr for HS1. For NEAP4K [*Rickaby and Elderfield*, 2005], we use the age model of *Lund et al.* [2015], which implies accumulation rates of ~5 cm/kyr for the LGM and ~3 cm/kyr for the deglaciation. For deep core KN166-14-JPC-13, we use the published age model, which suggests a timing of ice rafting and $\delta^{13}C$ decrease consistent with other North Atlantic cores [*Hodell et al.*, 2010], and accumulation rates of ~11 cm/kyr for the LGM and ~5 cm/kyr for the early deglaciation. We tie the nearly identical benthic $\delta^{13}C$ record from the other deep North Atlantic core, U1308 [*Hodell et al.*, 2008], to that of KN166-14-JPC-13 (supporting information Table S6 and Figure S4), implying accumulation rates of 4 cm/kyr for the LGM and 6 cm/kyr for the deglaciation. With these age models, the $\delta^{18}O_{BF}$ decrease in shallow (<2000 m) North Atlantic cores leads that of the deeper cores, consistent with previous results using different cores on age models derived with a different set of assumptions [*Waelbroeck et al.*, 2011]. Our timescales, especially for the subpolar North Atlantic cores, are subject to revisions in reservoir age estimates.

For our LGM compilation (supporting information Table S7), we use data from 22 to 20 kyr B.P. For our HS1 compilation, we use data from 17 to 15 kyr B.P. Assuming reasonable chronologies, the relatively short time interval of 2 kyr ensures that data from the different sites represent approximately the same interval, an important consideration given that $\delta^{18}O_{BF}$, and to a lesser extent $\delta^{13}C$, changed over the course of HS1 [e.g., *Waelbroeck et al.*, 2011]. However, previous work suggests that our first-order results are not sensitive to the precise interval of HS1 selected [*Oppo and Curry*, 2012; *Tessin and Lund*, 2013]. Furthermore, as our results do not hinge on results from a single core, they are likely robust against reasonable (±~500 years) chronological uncertainty.

### 3.1. EW9302 Isotope Records

EW9302 records are shown against age with two other records from similar water depths, NEAP4k, and ODP 984 (Figure 1). All EW9302 $\delta^{18}O_{BF}$ records have similar glacial and early deglacial values. While ODP 984 glacial values are similar to those of EW9302, of the two ODP 984 data points that fall between 17 and 15 kyr B.P., one has a much lower value and appears spurious. NEAP4k is offset to lower values for the whole of the LGM and early deglaciation. As the EW9302 (and ODP 984) data were generated in the same laboratory as much of the Brazil Margin data, and there are no offsets between the Brazil Margin data measured at WHOI and University of Michigan [*Tessin and Lund*, 2013; *Hoffman and Lund*, 2012], we assume that the EW9302 records are more directly comparable to the Brazil Margin data.

## 4. LGM and HS1 $\delta^{18}O_{BF}$ and $\delta^{13}C$ Profiles

Subpolar North Atlantic (red) and Brazil Margin (blue) depth profiles of $\delta^{13}C$ and $\delta^{18}O_{BF}$ for the LGM, HS1, and the HS1-LGM differences highlight some of the more salient differences between the LGM and HS1 (Figure 2).

LGM Brazil Margin $\delta^{18}O_{BF}$ data show a gradual increase with depth, whereas North Atlantic data are more homogenous (Figure 2a). With the exception of NEAP4k, North Atlantic $\delta^{18}O_{BF}$ values are higher than Brazil Margin values between 1300 and 1600 m, suggesting that the water at the shallow subpolar North Atlantic sites, on the east flank of the Reykjanes Ridge, was colder and/or saltier than water on the Brazil

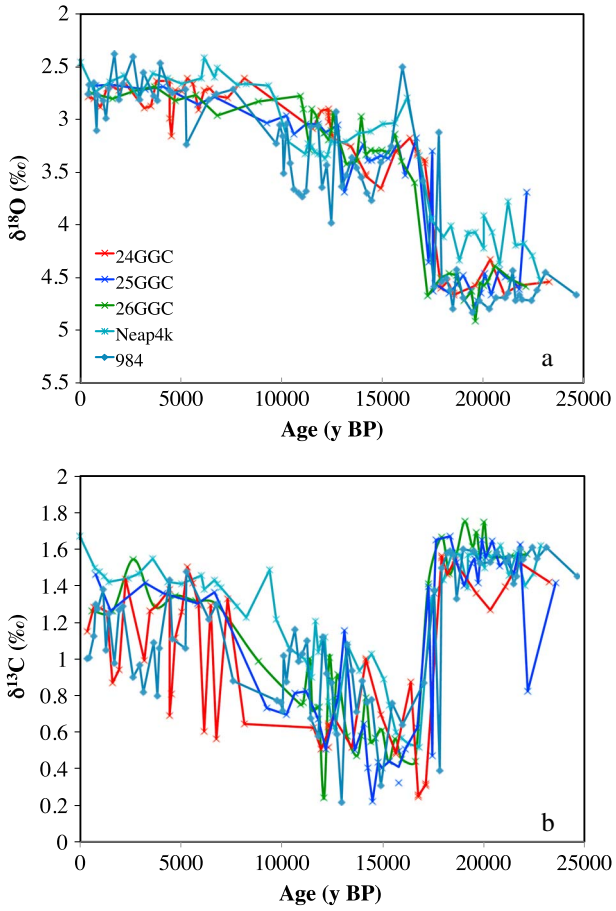


**Figure 1.** (a and b) Benthic $\delta^{13}C$ and $\delta^{18}O$ for ODP 984, NEAP4k, and EW9302 cores (Table 1) versus age. Data and age models for EW9302 cores are provided in supporting information Tables S1 and S2, respectively.

Margin at these depths. Between ~3000 and 4000 m, Brazil Margin values are higher than North Atlantic values, consistent with evidence of higher deep Southern Ocean salinity during the LGM [*Adkins et al.*, 2002].

As noted previously, the shallowest core (~1270 m) on the Brazil Margin included here was within the NADW/AAIW transition zone during the LGM and has lower $\delta^{13}C$ values than cores above (not shown) and below this depth [*Curry and Oppo*, 2005]. The inference of glacial low-$\delta^{13}C$ AAIW at this depth is bolstered by $\delta^{13}C$ data from other cores [*Curry and Oppo*, 2005], including one core with radiocarbon dates [*Lund et al.*, 2015], and by Cd/Ca data [*Makou et al.*, 2010]. Below this core depth, $\delta^{13}C$ decreases with depth on the Brazil Margin. LGM $\delta^{13}C$ also decreases with depth in the subpolar North Atlantic. Strong vertical $\delta^{13}C$ gradients occur between 2300 and 1650 m in the North Atlantic and between 2400 and 1800 m on the Brazil Margin (Figure 2d). LGM $\delta^{13}C$ values are higher in the North Atlantic than Brazil Margin throughout the cores' depth range.

There is no evidence of a low-$\delta^{13}C$ AAIW-like water mass influencing the ~1270 m Brazil Margin site during HS1 (Figure 2e). Instead, Brazil Margin $\delta^{13}C$ values decrease with depth, with a possible reversal of the $\delta^{13}C$ gradient just above 4000 m. Above ~2150 m, North Atlantic HS1 $\delta^{13}C$ values are relatively homogenous and higher (0.57 ± 0.04‰) than below 2150 m (0.15 ± 0.05‰) (Unless otherwise noted, errors reported are ±1 standard error). HS1 North Atlantic and Brazil Margin $\delta^{13}C$ values are similar at every depth.

Nearly homogeneous North Atlantic $\delta^{18}O_{BF}$ values during the LGM contrast with a $\delta^{18}O_{BF}$ gradient above 2300 m during HS1 (~0.7–1‰ range between shallowest cores and 2300 m, depending on which shallow cores are used to estimate properties of shallow water). Whereas the range of $\delta^{18}O_{BF}$ values on the Brazil Margin, between the shallowest core (~1270 m) and the deepest cores (~3600–3900 m), is similar for the LGM (0.9‰) and HS1 (~0.8–1.0‰, depending on which of the two deepest cores is used), the shapes of the profiles are different, with much of the $\delta^{18}O_{BF}$ increase occurring over a short depth interval (2100–2500 m) during HS1 compared to a gradual increase with depth during the LGM. Note the high Brazil Margin HS1 $\delta^{18}O_{BF}$ value at ~1600 m (second shallowest core) relative to cores above and below that depth is likely caused by bioturbation, as indicated by significant radiocarbon reversals [*Tessin and Lund*, 2013]. The north-south $\delta^{18}O_{BF}$ gradient above ~1650 m is reversed during HS1 relative to the LGM, and North Atlantic values are lower than Brazil Margin values throughout the depth range of our cores (~1300–4000 m) during HS1 (Figure 2a versus Figure 2b).

### 4.1. HS1-LGM $\delta^{18}O_{BF}$ and $\delta^{13}C$ Differences

The largest LGM-to-HS1 $\delta^{18}O_{BF}$ decrease (1.24 ± 0.04‰) occurred in shallow North Atlantic cores (EW9302 cores and RAPiD-10-1P, ~1240–1630 m) with decreasing amplitude with increasing water depth (Figure 2c).

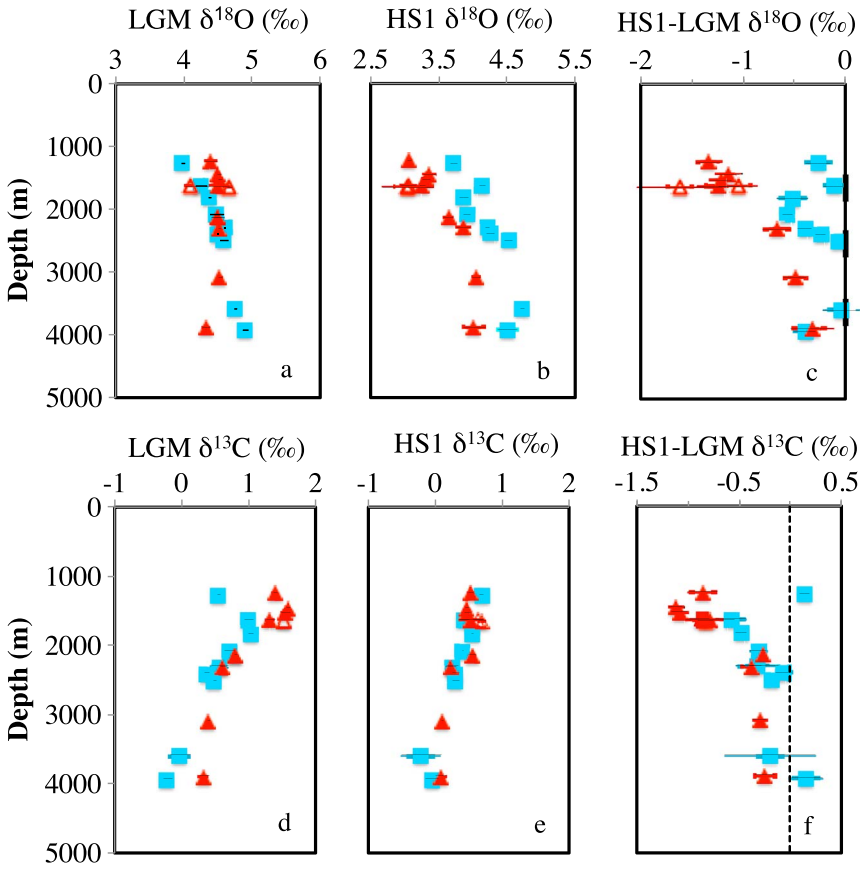


**Figure 2.** Depth profiles of (a) LGM $\delta^{18}O_{BF}$, (b) HS1 $\delta^{18}O_{BF}$, (c) the HS1-LGM $\delta^{18}O_{BF}$ difference, (d) LGM $\delta^{13}C$, (e) HS1 $\delta^{13}C$, and (f) the HS1-LGM $\delta^{13}C$ difference, with standard errors. Data denoted in red and blue are from North Atlantic (49°N–65°N) and Brazil Margin (27°S–30°S), respectively (Table 1). Open red symbols denote ODP 984 and NEAP4k data. Vertical line in Figure 2f denotes the zero line. Data plotted are provided in supporting information Table S7.

On the Brazil Margin, the HS1-LGM $\delta^{18}O_{BF}$ difference was largest in cores between ~1800 and 2000 m, with smaller differences both above and below that depth. (Note, however, that the small change at the ~1600 m depth Brazil Margin site is due to the anomalous HS1 $\delta^{18}O_{BF}$ values for that depth). The LGM-to-HS1 $\delta^{18}O_{BF}$ decrease was greater in the North Atlantic than at the Brazil Margin at all but the deepest core sites (Figure 2c).

Like $\delta^{18}O_{BF}$, the largest LGM-HS1 $\delta^{13}C$ decrease ($0.96 \pm 0.08$‰) occurred in shallow North Atlantic cores (EW9302 cores and RAPiD-10-1P, ~1240–1630 m) (Figure 2f). Also, like $\delta^{18}O_{BF}$, the LGM-HS1 $\delta^{13}C$ decrease was greater in the shallower than deeper Brazil Margin cores. In general, the higher the $\delta^{13}C$ value during the LGM, the larger the LGM-HS1 $\delta^{13}C$ decrease ($R^2 = 0.9$) (Figure 3). Only data from the shallowest Brazil Margin core (KNR159-5-36GGC, ~1270 m) strongly influenced by AAIW during the LGM fall off the trend and are not included in the linear regression. Sites with larger LGM-HS1 $\delta^{13}C$ decreases tend to be associated with larger $\delta^{18}O_{BF}$ decreases (Figure 4, $R^2 = 0.75$; we exclude ODP 984 (~1650 m) and KNR159-5-17JPC (~1600 m) because they have anomalous HS1 $\delta^{18}O_{BF}$ values for their water depths).

Two robust features emerge from our analysis of the LGM and HS1 $\delta^{18}O_{BF}$ and $\delta^{13}C$ data—the correspondence between the LGM $\delta^{13}C$ value and the LGM-HS1 $\delta^{13}C$ difference and between the LGM-HS1 $\delta^{13}C$ and $\delta^{18}O_{BF}$ changes (Figures 3 and 4). Thus, any explanation for the early deglacial $\delta^{13}C$ must explain these features and must also explain why the $\delta^{13}C$ change at site KNR159-5-36GGC (~1270 m) within glacial AAIW was relatively small compared to its LGM value.

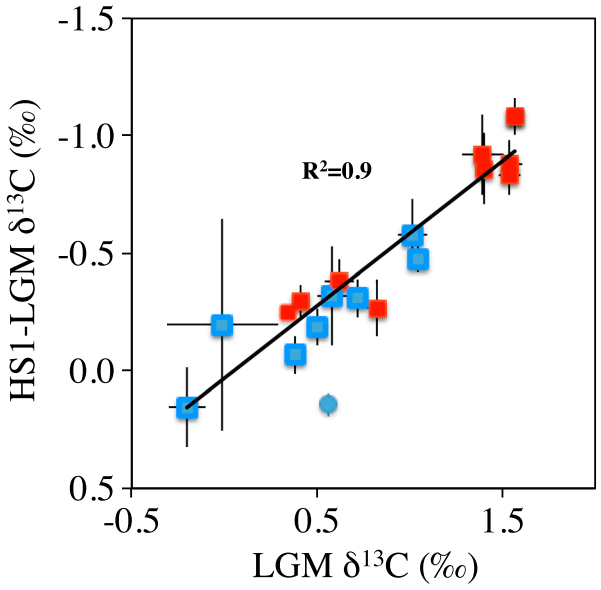


**Figure 3.** LGM $\delta^{13}C$ versus HS1-LGM $\delta^{13}C$. North Atlantic and Brazil Margin data are in red and blue, respectively. Blue circle denotes the AAIW depth Brazil Margin core (KNR159-5-36GGC). Error bars represent ±1 standard error.

## 5. Water Mass Mixing

### 5.1. The LGM

North Atlantic LGM $\delta^{18}O_{BF}$ values are nearly constant, but $\delta^{13}C$ decreases with depth (Figure 2d), trending from high-$\delta^{13}C$ NADW to a lower $\delta^{13}C$ southern sourced water mass (Figure 5; black line). Data from North Atlantic cores below 2100 m overlap LGM Brazil Margin data from 1800 to 2400 m depth cores (Figure 5; green line), implying similar NADW:SOW mixtures bathed the sites.

LGM Brazil Margin data from 1600 to 4000 m fall along a mixing line that extends from a deep end-member, having high $\delta^{18}O_{BF}$ and low $\delta^{13}C$ values, to a shallower end-member, having lower $\delta^{18}O_{BF}$ and higher $\delta^{13}C$ values ($R^2 = 0.9$; Figure 5). Because of the influence of low-$\delta^{13}C$ glacial AAIW [*Curry and Oppo*, 2005], the Brazil Margin point from ~1260 m has low $\delta^{13}C$ values for its water depth (Figure 2d) and falls off the trend defined by data from deeper cores (Figure 5, green triangle). The mixing trend implied by the deep Brazil Margin data projects below shallow North Atlantic data, likely due to the contribution of low-$\delta^{13}C$ glacial AAIW.

### 5.2. HS1 North Atlantic

HS1 North Atlantic data (Figure 5, blue symbols) fall along a mixing line trending from a shallow, relatively low-$\delta^{18}O_{BF}$, high-$\delta^{13}C$ water mass—presumably NADW—to a deeper, high-$\delta^{18}O_{BF}$, low-$\delta^{13}C$ water mass ($R^2 = 0.84$). If we omit data from RAPiD-15-4P (~2100 m), which falls off the mixing trend and may have a high $\delta^{13}C$ for its water depth (Figure 2e, fourth point from the bottom), then $R^2 = 0.96$. Assuming for the moment that the three shallowest cores lie within HS1 NADW, we estimate HS1 NADW source values of 3.25 ± 0.16‰ (1 standard deviation) and 0.50 ± 0.03‰ for $\delta^{18}O_{BF}$ and $\delta^{13}C$, respectively. The HS1 North Atlantic mixing line projects to the deep Brazil Margin data (Figure 5, orange symbols), consistent with a common southern end-member as suggested by numerous studies (section 2.4). Lower HS1 $\delta^{18}O_{BF}$ values in the deep North Atlantic than deep Brazil Margin (Figures 2b and 5) indicate that deep North Atlantic waters were warmer and/or had lower $\delta^{18}O_{SW}$.

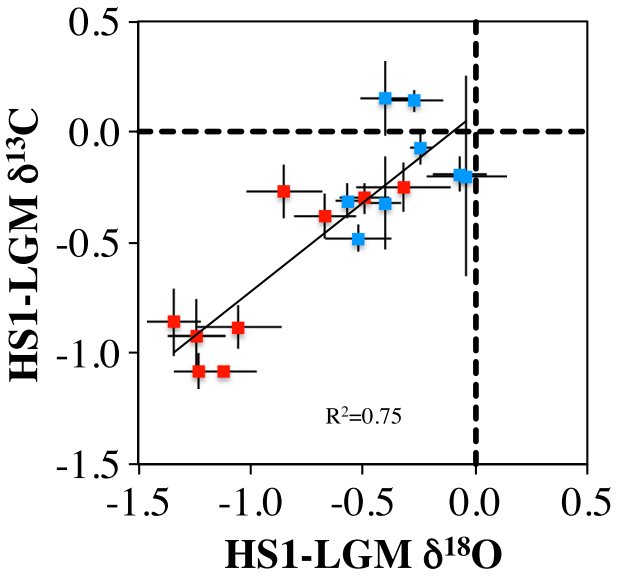


**Figure 4.** HS1-LGM $\delta^{18}O_{BF}$ versus $\delta^{13}C$ differences, with North Atlantic data in red, and Brazil Margin data in blue (Tables 1 and S7 in the supporting information). Error bars represent ±1 standard error. Data from ODP 984 (~1650 m) and KNR159-5-17JPC (~1600 m) are not shown or included in the regression, because they have anomalous HS1 $\delta^{18}O_{BF}$ values for their water depths (Figure 2b).

### 5.3. HS1 Brazil Margin

During HS1, and in contrast to the LGM, data from the core within the depth of modern and LGM AAIW (KNR159-5-36GGC, ~1270 m; red triangle, Figure 5), fall along the same

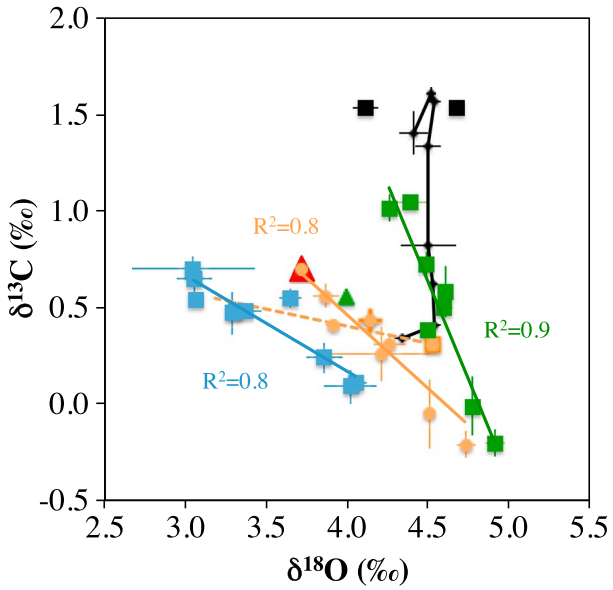


**Figure 5.** The $\delta^{18}O_{BF}$ versus $\delta^{13}C$ for the LGM North Atlantic (black), LGM South Atlantic (green), HS1 North Atlantic (blue), and HS1 South Atlantic (orange). The black line connecting the LGM North Atlantic data extends from the shallowest to the deepest core. Solid black squares denote LGM values from NEAP4K and ODP 984. Linear regressions of the other data sets are shown by solid lines of the same color. During the LGM, data from the AAIW depth core (KNR159-5-36GGC; green triangle) falls off the mixing line and is not included in the regression. During HS1, data from KNR159-5-36GGC (red triangle) falls along the mixing line describing the deeper data. The dashed orange line extends from the data from the 2500 m Brazil Margin core (KNR159-5-30GGC; orange square) to data from the shallow North Atlantic cores. The North Atlantic HS1 point that falls off the regression is RAPiD-15-4P, which is, however, included in the regression. Error bars represent ±1 standard error. Data sources and data provided in Table 1 and Table S1 in the supporting information, respectively.

mixing line defined by data from deeper Brazil Margin cores (Figure 5; solid orange line, $R^2 = 0.82$). Thus, it does not appear that a shallow relatively low-$\delta^{13}C$ AAIW-like water mass influenced the Brazil Margin during HS1. Although most of the Brazil Margin data from cores between ~1270 and 4000 m fall along a single mixing line, they do not project toward the cluster of shallow North Atlantic data points (Figure 5), suggesting that two-component mixing between a middepth (~1230–1650 m) subpolar North Atlantic water mass and the water mass at the deepest Brazil Margin sites does not adequately describe the data.

Whereas we only have data from one Brazil Margin core in the 2500–3000 m depth range, *Lund et al.* [2015] present two new isotope records from ~2700 and 2950 m, filling a critical gap. Like the data from the ~2500 m depth core included here and plotted as a solid orange square (Figure 5), the new HS1 data (not shown) fall closer to the LGM Brazil Margin mixing line and above the HS1 Brazil shallow-to-deep mixing line (Figure 5). *Lund et al.* [2015] suggest that the Brazil Margin data from cores above 2500 m can be described by a line with a relatively shallow slope, extending from data from 2500 to 3000 m cores to the values from the shallow North Atlantic sources (approximated by dashed orange line, which extends from data from the 2500 m depth core; Figure 5). Moreover, they conclude that water at the deepest Brazil Margin sites (below 3000 m) was isolated from North Atlantic influence until after the end of HS1, consistent with evidence from the deep eastern South Atlantic [*Waelbroeck et al.*, 2011; *Yu et al.*, 2014].

The mixing line trending from Brazil Margin data to data from shallow North Atlantic cores (dashed orange line in Figure 5) implies that NADW, having source values described by these shallow North Atlantic cores, influenced the Brazil Margin [*Lund et al.*, 2015]. It further implies that the LGM-HS1 $\delta^{13}C$ decrease was largely caused by a decrease in the source value of NADW from its LGM value, rather than a NADW fraction decrease. While this may have been the case, and we discuss this possibility in section 6, we note that shallower Brazil Margin data fall above the hypothesized mixing trend. Thus, in this scenario, a third relatively shallow water mass must have mixed into the region. For example, southward flowing NADW may have mixed with overlying higher $\delta^{13}C$, lower $\delta^{18}O_{BF}$ (fresher and/or warmer) North Atlantic deep thermocline water (consistent with HS1 values from the Florida Margin [*Lynch-Stieglitz et al.*, 2014]). Alternatively or in addition, relatively shallow southern sources mixing into the region may have pulled Brazil Margin values away from the NADW source values.

## 6. The LGM-HS1 $\delta^{13}C$ Decrease

Mechanisms that might contribute to a $\delta^{13}C$ decrease at depth in the ocean include (1) local accumulation of low-$\delta^{13}C$ remineralized carbon, (2) a reduction in the $\delta^{13}C$ value of one or more sources filling the ocean's interior, and (3) a decrease in the fraction of a relatively high $\delta^{13}C$ water mass such as NADW.

**Table 2.** End-Member Values (Mean ± 1 Standard Deviation)

| | LGM | | HS1 | |
|---|---|---|---|---|
| | $\delta^{18}O_{BF}$ | $\delta^{13}C$ | $\delta^{18}O_{BF}$ | $\delta^{13}C$ |
| NADW | 4.48 ± 0.07 | 1.51 ± 0.09 | 3.25 ± 0.16 | 0.50 ± 0.03 |
| Deep South Atlantic | 4.84 ± 0.10 | −0.11 ± 0.13 | 4.62 ± 0.15 | −0.13 ± 0.16 |

First, we consider the possible influence of accumulation of locally respired carbon on the LGM-to-HS1 $\delta^{13}C$ decrease. The observation that data from Brazil Margin cores having the largest $\delta^{13}C$ change (from ~1800 and 2100 m) do not have lower values during HS1 than cores above or below that depth (Figure 2e) suggests that local accumulation of respired carbon did not contribute significantly to the LGM-to-HS1 $\delta^{13}C$ decrease on the Brazil Margin. Data from these sites also fall along or close to mixing lines between shallower and deeper data, whether extending from the 2500 m core or from the deepest cores (dashed and solid orange lines, respectively, Figure 5), without systematic departures to low $\delta^{13}C$ values, also consistent with conservative mixing. However, as we discuss in section 7, the relatively low $\delta^{13}C$ values of the shallow North Atlantic sites may suggest that the North Atlantic contained a larger fraction of "old" water containing respired carbon during HS1.

Second, we consider a reduction in the NADW $\delta^{13}C$ source value as the cause of the LGM-to-HS1 $\delta^{13}C$ decrease (e.g., dashed orange line, Figure 5). If the shallow North Atlantic sites were situated to sample the HS1 NADW end-member, then the entire LGM-to-HS1 $\delta^{13}C$ decrease at these same sites (~1‰; Table 2) must have been due to a decrease in the NADW source value, with no decrease in the NADW fraction. To illustrate the influence of an ~1‰ decrease in the NADW end-member, with no change in the volume of NADW in the Atlantic, we consider three hypothetical locations, containing 80%, 50%, and 30% NADW during the LGM. The LGM $\delta^{13}C$ value for these sites is determined by assuming two-component mixing between the high-$\delta^{13}C$ North Atlantic and low-$\delta^{13}C$ deep South Atlantic end-members, using $\delta^{13}C$ values indicated in Table 2. As already noted, during the LGM, Brazil Margin data project below the shallow North Atlantic end-member (Figure 5), presumably because of the presence of a third low-$\delta^{13}C$ end-member (glacial AAIW), so our assumption of two-component mixing overestimates the LGM %NADW at the shallower Brazil Margin sites. Ignoring this complication, we estimate that changes in the NADW source value alone, with no change in the fraction of NADW to our sites, would cause $\delta^{13}C$ to decrease by 0.8, 0.5, and 0.3‰ at the three hypothetical locations, respectively (Figure 6, blue squares) consistent with the observed relationship between LGM $\delta^{13}C$ and the LGM-HS1 $\delta^{13}C$ decrease (Figure 6, orange circles).

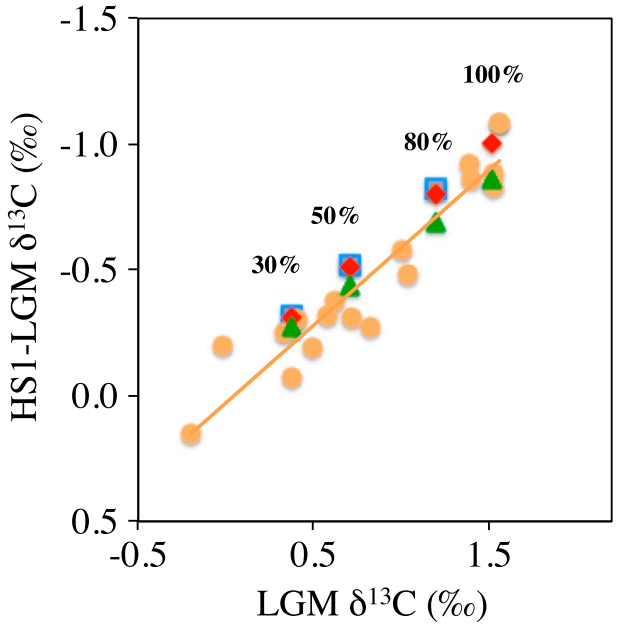


**Figure 6.** LGM $\delta^{13}C$ versus HS1-LGM $\delta^{13}C$. Orange symbols indicate the North Atlantic and Brazil Margin data. Blue squares show the predicted $\delta^{13}C$ change for waters at three hypothetical sites containing 80%, 50%, and 30% NADW during the LGM, assuming only a NADW $\delta^{13}C$ source change, that is, with no change in the NADW fraction. Higher LGM $\delta^{13}C$ values correspond to higher LGM %NADW, as described in text. Overlying red diamonds show the $\delta^{13}C$ change for these same hypothetical sites, assuming no change in the NADW source value, only a change in the fraction of NADW at these sites. Red diamond below the 100% label shows the $\delta^{13}C$ change for both of these scenarios at a site containing 100% NADW during the LGM (e.g., at a $\delta^{13}C$ of 1.52‰). Green triangles show the predicted $\delta^{13}C$ change at these same sites assuming half of the $\delta^{13}C$ decrease at the North Atlantic sites (~0.5‰) was due to a change in the NADW source value, and the other half due to a 30% reduction in the fraction of NADW.

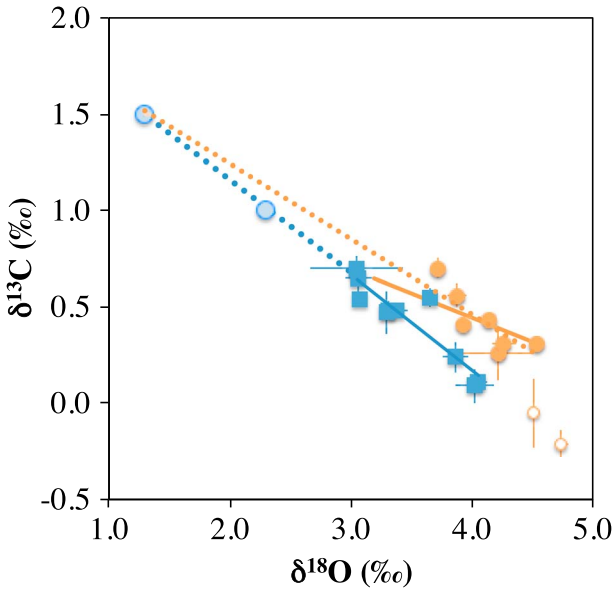


**Figure 7.** The $\delta^{18}O_{BF}$ versus $\delta^{13}C$ for HS1. North Atlantic data and Brazil Margin data are plotted in blue squares and orange circles, respectively. Open orange symbols denote data from the two deepest Brazil Margin sites. The solid orange line extends from the values from the 2500 m Brazil Margin core (KNR159-5-30GGC; orange square) to values from the shallow North Atlantic cores. This mixing line assumes that the entire $\delta^{13}C$ change at the shallow North Atlantic sites was due to a NADW source change. Light blue circles denote hypothetical NADW end-member values if the NADW $\delta^{13}C$ source value was the same as the LGM (point at $\delta^{13}C \sim 1.5‰$), or if half of the $\delta^{13}C$ decrease at the shallow North Atlantic sites was due to a decrease in the NADW source values (point at $\delta^{13}C = 1‰$).

We consider the alternative extreme that the "true" HS1 $\delta^{13}C$ end-member was the same as the LGM end-member value (1.5‰; Table 2) and that the entire $\delta^{13}C$ decrease in the shallow North Atlantic sites was due to a decrease in the NADW water mass fraction. We project the North Atlantic mixing line to the alternative, higher $\delta^{13}C$ end-member value to estimate the North Atlantic end-member $\delta^{18}O_{BF}$ value (~1.3‰) (Figure 7). A linear regression fit to this point and the Brazil Margin data from cores 2500 m and shallower describes a NADW-South Atlantic mixing line (Figure 7, dotted orange line; $R^2 = 0.9$; $R^2 = 0.7$ if the North Atlantic end-member value is not included). Using the LGM North Atlantic end-member $\delta^{13}C$ value of 1.5‰ as our HS1 NADW end-member value, and the observed HS1 deep South Atlantic value (−0.11‰, Table 2) as our southern end-member, we estimate that the shallow North Atlantic core sites, where HS1 $\delta^{13}C$ was approximately 0.5‰ (Table 2), contained ~40% NADW, or a 60% reduction from the LGM. Using these same $\delta^{13}C$ end-member values, we estimate the effect of a 60% reduction in the fraction of NADW on HS1 $\delta^{13}C$ and the LGM-HS1 $\delta^{13}C$ change at our same hypothetical sites containing 80%, 50%, and 30% NADW during the LGM (red diamonds, Figure 6). The predicted $\delta^{13}C$ decreases overlie those decreases predicted by assuming only a decrease in the North Atlantic source value.

These illustrations clarify that we can explain the entire $\delta^{13}C$ decrease by either a reduction in the source value only or by an ~60% reduction in NADW fraction only. Both these mechanisms decrease the $\delta^{13}C$ values more at sites having high %NADW during the LGM, consistent with the data (Figure 6). Of course, we can also explain the $\delta^{13}C$ decrease by a combination of the two mechanisms—for example, by a 0.5‰ decrease in the NADW source value (a HS1 $\delta^{13}C$ end-member of 1.0‰) and a 30% reduction in the fraction of NADW (Figure 6, green triangles).

The low-$\delta^{18}O_{BF}$ signal during HS1 appears to be associated with a shallow North Atlantic source, as it seems unlikely to have originated from below, or from the south (Figure 2b). In these scenarios, the locations with the greatest NADW fraction during the LGM, as determined from $\delta^{13}C$, would also have the greatest fraction during HS1, so $\delta^{18}O_{BF}$ would have decreased most at these sites consistent with the evidence that larger $\delta^{13}C$ decreases were generally accompanied by larger $\delta^{18}O_{BF}$ decreases (Figure 4). However, as we discuss in section 7, the low $\delta^{18}O_{BF}$ values on the Brazil Margin may not have been uniquely associated with the HS1 NADW end-member.

Both scenarios are also consistent with the $\delta^{13}C$ change at the depths of LGM AAIW (Figure 3, blue circle). During the LGM, isotopic values from core KNR159-5-36GGC (~1270 m) fall far from the mixing line that describes the deeper data, suggesting that the fraction of NADW at the core site was small during the LGM. Thus, neither a decrease in the NADW source value nor a decrease in the fraction of NADW to the site would cause $\delta^{13}C$ to decrease there. Rather, the $\delta^{13}C$ was higher at the core site during HS1 than during the LGM, likely because low-$\delta^{13}C$ glacial AAIW was replaced by a higher-$\delta^{13}C$ source during HS1.

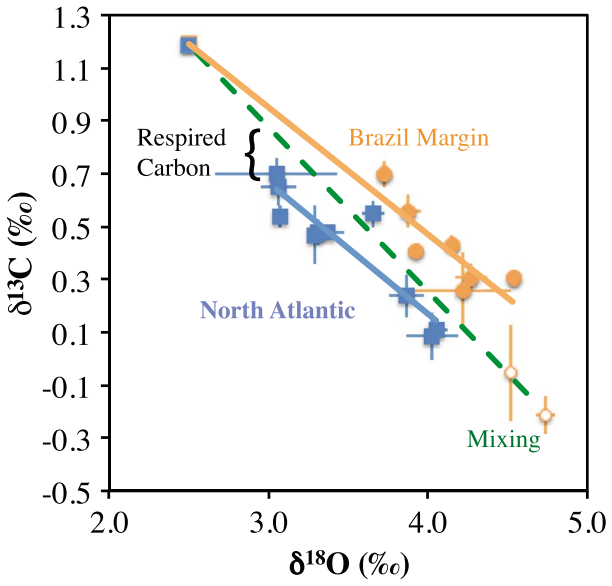


**Figure 8.** The $\delta^{18}O_{BF}$ versus $\delta^{13}C$ for HS1. North Atlantic data and Brazil Margin data are plotted in blue squares and orange circles, respectively. Open orange symbols denote data from the two deepest Brazil Margin sites. The linear regression through the ≤2500 m Brazil Margin data is extended to a hypothetical shallow North Atlantic source (blue square). Green dashed line denotes mixing between deep Brazil Margin and the hypothetical shallow North Atlantic end-member. Bracket denotes the effect of accumulated respired carbon in reducing $\delta^{13}C$ values at the shallower North Atlantic core sites.

Results of a model simulation of a multimillennial-long AMOC shutdown, forced by adding freshwater to a surface North Atlantic preindustrial control, suggest that an AMOC shutdown would dramatically reduce the contribution of high-$\delta^{13}C$ North Atlantic surface water to depth and result in greater accumulation of respired carbon in the subpolar North Atlantic [*Schmittner and Lund*, 2015], similar to an earlier transient simulation using a zonally averaged model [*Marchal et al.*, 1998]. We consider it likely that as in the simulations, the LGM-to-HS1 $\delta^{13}C$ decrease at the shallow North Atlantic sites was at least in part due to poorer ventilation by North Atlantic surface water and greater accumulation of respired carbon, in response to a weaker AMOC. An example of how the HS1 data might fit with this scenario is illustrated in Figure 8; we arbitrarily extend the regression through the Brazil Margin data from cores 2500 m and shallower to a $\delta^{13}C$ values of ~1.2‰ and assume this to be the North Atlantic end-member value. At any given $\delta^{18}O_{BF}$ value, the $\delta^{13}C$ difference between the observed North Atlantic mixing line (blue) and the mixing line between the hypothetical North Atlantic end-member and the deep Brazil Margin (green dashed line) reflects the influence of respired carbon on North Atlantic $\delta^{13}C$. Assuming this end-member value, 0.3‰ of the 1‰ LGM-HS1 $\delta^{13}C$ decrease at the shallow North Atlantic sites is due to NADW source water change (allowing for some decrease, for example, due to the lower atmospheric $\delta^{13}C$ value [*Schmitt et al.*, 2012] and reduced air-sea gas exchange [*Waelbroeck et al.*, 2011]), 0.2‰ to the contribution of accumulated respired carbon, and 0.5‰ to a decrease in the NADW fraction. However, the actual contribution of these three processes is poorly constrained by the data. Like the NADW fraction-only scenario (but unlike the source-only change scenario), this scenario implies that the main southward flow of northern sourced waters occurred above the shallowest North Atlantic core sites and that this North Atlantic water mass was an important component of the shallow, low-$\delta^{18}O_{BF}$, high-$\delta^{13}C$ end-member on the Brazil Margin (Figure 8).

## 7. Discussion

Based on the North Atlantic and Brazil Margin $\delta^{18}O_{BF}$ versus $\delta^{13}C$ lines (Figures 5 and 8), we infer that during HS1, a deep, relatively high-$\delta^{18}O_{BF}$, low-$\delta^{13}C$ water mass flowed from the south to the North Atlantic. To what extent North Atlantic sourced water flowed southward in the upper limb of the AMOC is uncertain, as it seems possible to explain the early deglacial $\delta^{13}C$ decrease that occurred throughout much of the upper Atlantic and deep North Atlantic by invoking either a large (1‰) decrease in the $\delta^{13}C$ of NADW without an increase in the fraction of NADW in the subsurface Atlantic or a significant reduction in the proportion (and hence volume) of NADW in the Atlantic, with no change in source value (Figure 6).

Although there may be alternate explanations for any single type of proxy record suggesting a reduced AMOC during HS1, many lines of evidence suggest a weaker AMOC, as discussed in section 2.4. Thus, our preferred explanation is that the LGM-to-HS1 $\delta^{13}C$ decrease that occurred throughout much of the upper (<2500 m) Atlantic and the deep North Atlantic was caused by a weaker, shallow AMOC, consistent with results from model simulations. A smaller contribution of high-$\delta^{13}C$ surface water to the shallow north Atlantic core sites implies a

greater contribution of older waters, either SOW or aged deep waters previously formed in the North Atlantic, or both, consistent with subpolar North Atlantic radiocarbon data [*Thornalley et al*., 2011]. If we accept that the deep South Atlantic was isolated during early HS1 [*Waelbroeck et al*., 2011; *Yu et al*., 2014; *Lund et al*., 2015], this scenario also allows us to take the mixing lines suggested by regressions through the North Atlantic and Brazil Margin $\delta^{18}O_{BF}$-$\delta^{13}C$ data at face value (Figure 8). As noted, however, this scenario implies that the southward flow of North Atlantic source waters occurred above our shallowest North Atlantic cores site (~1250 m), which does not sample the true HS1 end-member. Is this consistent with the $\delta^{18}O_{BF}$ data?

The strongest vertical $\delta^{18}O_{BF}$ gradients during HS1 were at approximately the same depth as the strongest vertical $\delta^{13}C$ gradients during the LGM (Figures 2b and 2e). In both the North and South Atlantic, vertical $\delta^{18}O_{BF}$ gradients during HS1 appear to separate two water masses, one above 2000 m and one below 2000 m, possibly implying similar water mass boundaries as the LGM [e.g., *Curry and Oppo*, 2005]. However, without constraints on the end-member properties of significant source waters filling the Atlantic, it is not possible to identify the depth of the core of southward flowing NADW from $\delta^{18}O_{BF}$ data or to determine whether the depth marking a specific NADW:SOW mixture (e.g., a 50:50 mixture) was at the same depth during HS1 as during the LGM.

Lower $\delta^{18}O_{BF}$ values in the deep North Atlantic than in the deep Brazil Margin (Figures 2b and 5) indicate that deep North Atlantic waters were warmer and/or had lower $\delta^{18}O_{SW}$, consistent with the presence of a NADW signal in the deep North Atlantic during HS1, as suggested in some previous studies [*Barker et al*., 2004; *Waelbroeck et al*., 2011]. As the surface North Atlantic appears to have been relatively fresh during HS1 due to ice melting [*Bond et al*., 1992], it is likely that a portion of the North Atlantic $\delta^{18}O_{BF}$ decrease was due to downward mixing of low-$\delta^{18}O$ deglacial surface water. Brines may have also contributed to the relatively low $\delta^{18}O_{BF}$ values [*Waelbroeck et al*., 2011]. However, some component of the $\delta^{18}O_{BF}$ decrease in the deep North Atlantic was likely due to warming, as weaker convection during HS1 would have resulted in the reduction of heat transferred from the surface to subsurface [e.g., *Liu et al*., 2009; *Marcott et al*., 2011]. Thus, we consider it likely that below the hypothesized shallow southward transport of North Atlantic waters during HS1, both downward mixing and warming contributed to the low deep North Atlantic $\delta^{18}O_{BF}$ values relative to the deep South Atlantic.

Above the lower boundary of the $\delta^{18}O_{BF}$ gradient (~2300 m) and below the level of active southward transport, low-$\delta^{18}O$ waters may have mixed along isopycnals to the South Atlantic, but local subsurface warming likely also contributed to the low $\delta^{18}O_{BF}$ values on the Brazil Margin. Similar to previous studies [e.g., *Manabe and Stouffer*, 1997], a transient deglacial simulation suggests that with a weaker (or collapsed) AMOC, heat previously transported to the North Atlantic accumulates in South Atlantic above ~2000 m [*Liu et al*., 2009]. Moreover, with deglacial warming underway in the Southern Hemisphere [e.g., *Jouzel et al*., 2001; *Barker et al*., 2009], waters originating at the surface would have transmitted a warming signal to depth. Thus, as in the North Atlantic [*Marcott et al*., 2011], some component of the HS1 $\delta^{18}O_{BF}$ decrease on the Brazil Margin may also reflect local warming.

Thus, we argue that even if the southward transport by NADW occurred shallower than during the LGM, an AMOC reduction would be consistent with a relatively deep $\delta^{18}O_{BF}$ gradient during HS1. We hypothesize that the ~2300 m lower boundary of the $\delta^{18}O_{BF}$ gradient indicates the depth to which the North Atlantic freshwater signal had mixed into the subsurface ocean, as well as the depths that had warmed most—both due to heat redistribution in response to a reduced AMOC and by direct ventilation of Southern Hemisphere surface waters, which were warming at the time [e.g., *Barker et al*., 2009]. This scenario is also consistent with the lead of the upper Atlantic deglacial $\delta^{18}O_{BF}$ decrease relative to deeper sites [e.g., *Waelbroeck et al*., 2011; *Lund et al*., 2015].

## 8. Conclusions

1. The $\delta^{13}C$ decrease that began approximately synchronously with HS1, found at many Atlantic sites above 2500 m and in the deep North Atlantic, can be explained entirely by a decrease in the NADW $\delta^{13}C$ source value, entirely by a decrease in the contribution of NADW relative to SOW, or by a smaller contribution from each.
2. Consistent with model simulations [*Schmittner and Lund*, 2015], however, we hypothesize that a weaker AMOC, which reduced ventilation by North Atlantic surface water, resulted in greater accumulation of

low-$\delta^{13}C$ respired carbon between ~1200 and 1650 m in the subpolar North Atlantic. The relative influence of greater accumulation of respired carbon in the North Atlantic, a possible decrease in the NADW $\delta^{13}C$ value by other mechanisms, and a lower fraction of northern source water, on the early deglacial $\delta^{13}C$ decrease is poorly constrained.

3. The lowest HS1 $\delta^{18}O_{BF}$ values occur in shallow North Atlantic cores and appear associated with a North Atlantic source. However, we argue that downstream of the North Atlantic, low $\delta^{18}O_{BF}$ is not uniquely a tracer of southward flowing NADW.
4. While low-$\delta^{18}O_{BF}$ northern source waters may have contributed to low $\delta^{18}O_{BF}$ values above 2500 m on the Brazil Margin, local warming due to a reduced AMOC and ventilation by relatively warm southern source waters may have also been factors.
5. Lower $\delta^{18}O_{BF}$ values in the deep North Atlantic compared to the deep Brazil Margin imply that deglacial freshwater mixed into the deep North Atlantic during HS1. Reduction of the heat source from local convection may have resulted in subsurface North Atlantic warming, also contributing to the relatively low North Atlantic $\delta^{18}O_{BF}$ values.
6. Rather than denote a boundary between southward flowing NADW above and northward flowing SOW below, we suggest that the relatively sharp vertical $\delta^{18}O_{BF}$ gradient during HS1, having a lower boundary near ~2500 m on the Brazil Margin and ~2300 m in the subpolar North Atlantic, may mark the division between upper waters most influenced by mixing of deglacial meltwater and heat by this time, and deeper waters less influenced by these processes.
7. There is no evidence of a low-$\delta^{13}C$ AAIW-like water mass on the Brazil Margin during HS1.

**Acknowledgments**

Data for the figures are available in the supporting information tables. Supporting data not already available through the World Data Center for Paleoclimatology or Pangaea will be posted at the Center. The work was supported by NSF grants OCE13-35191, OCE07-50880, and OCE05-84911 to the Woods Hole Oceanographic Institution. We thank S. Praetorius, L. Zou, and M. Jeglinski for laboratory assistance; G. Gebbie, D. Lund, O. Marchal, and D. Thornalley for comments on the manuscript and/or discussions; O. Marchal for making Figure S1; D. Lund and A. Schmittner for sharing their unpublished manuscripts; two anonymous reviewers for their insightful reviews; and Chris Charles for his handling of the manuscript.

## References

Adkins, J. F. (2013), The role of deep ocean circulation in glacial to interglacial climate change, *Paleoceanography*, *28*, 1–23, doi:10.1002/palo.20046.

Adkins, J. F., K. McIntyre, and D. P. Schrag (2002), The salinity, temperature and $\delta^{18}O$ content of the glacial deep ocean, *Science*, *298*, 1769–1773.

Bainbridge, A. (1981), *GEOSECS Atlantic Expedition, Hydrographic Data Volume 1*, US Government Printing Office, Washington, D. C.

Barker, S., T. Kiefer, and H. Elderfield (2004), Temporal changes in North Atlantic circulation constrained by planktonic foraminiferal shell weights, *Paleoceanography*, *19*, PA3008, doi:10.1029/2004PA001004.

Barker, S., P. Diz, M. J. Vautravers, J. Pike, G. Knorr, I. R. Hall, and W. S. Broecker (2009), Interhemispheric Atlantic seesaw response during the last deglaciation, *Nature*, *457*, 1097–1102.

Belanger, P. E., W. B. Curry, and R. K. Matthews (1981), Core-top evaluation of benthic foraminiferal isotopic ratios for paleo-oceanographic interpretations, *Palaeogeogr. Palaeoclimatol. Palaeoecol.*, *33*, 221–231.

Bemis, B. E., H. J. Spero, J. Bijma, and D. W. Lea (1998), Reevaluation of the oxygen isotopic composition of planktonic foraminifera: Experimental results and revised paleotemperature estimates, *Paleoceanography*, *13*, 150–160, doi:10.1029/98PA00070.

Bond, G. C., et al. (1992), Evidence for massive discharges of icebergs into the North Atlantic Ocean during the last glacial, *Nature*, *360*, 245–249.

Boyle, E. A., and L. D. Keigwin (1987), North Atlantic thermohaline circulation during the past 20,000 years linked to high-latitude surface temperature, *Nature*, *330*, 35–40.

Bradtmiller, L. S., J. F. McManus, and L. F. Robinson (2014), 231Pa/230Th evidence for a weakened but persistent Atlantic meridional overturning circulation during Heinrich Stadial 1, *Nat. Commun.*, *5*, 5817.

Broecker, W. S., and E. Maier-Reimer (1992), The influence of air and sea exchange on the carbon isotope distribution in the sea, *Global Biogeochem. Cycles*, *6*(3), 315–320, doi:10.1029/92GB01672.

Burke, A., O. Marchal, L. I. Bradtmiller, J. F. McManus, and R. François (2011), Application of an inverse method to interpret $^{231}Pa/^{230}Th$ observations from marine sediments, *Paleoceanography*, *26*, PA1212, doi:10.1029/2010PA002022.

Came, R. E., D. W. Oppo, and W. B. Curry (2003), Atlantic Ocean circulation during the Younger Dryas: Insights from a new Cd/Ca record from the western subtropical South Atlantic, *Paleoceanography*, *18*, 1086, doi:10.1029/2003PA000888.

Came, R. E., W. B. Curry, D. W. Oppo, A. J. Broccoli, and R. J. Stouffer (2007), North Atlantic intermediate depth variability during the Younger Dryas: Evidence from benthic foraminiferal Mg/Ca and the GFDL R30 coupled climate model, in *Ocean Circulation: Mechanisms and Impacts*, *Geophys. Monogr. Ser.*, vol. 173, edited by A. Schmittner, J. Chiang, and S. Hemmings, pp. 247–264.

Came, R. E., D. W. Oppo, W. B. Curry, and J. Lynch-Steiglitz (2008), Variability in the influence of Antarctic Intermediate Water in the Florida Current over the last 20,000 years, *Paleoceanography*, *23*, PA1217, doi:10.1029/2007PA001450.

Chase, Z., R. F. Anderson, M. Q. Fleisher, and P. W. Kubik (2002), The influence of particle composition and particle flux on scavenging of Th, Pa and Be in the ocean, *Earth Planet. Sci. Lett.*, *204*, 215–229.

Craig, H., and L. I. Gordon (1965), Deuterium and oxygen 18 variations in the ocean and the marine atmosphere, in *Stable Isotopes in Oceanographic Studies and Paleotemperatures*, edited by E. Tongiori, pp. 9–131, Laboratorio di Geologia Nucleare, Pisa, Italy.

Curry, W. B., and D. W. Oppo (2005), Glacial water mass geometry and the distribution of $\delta^{13}C$ of $\Sigma CO_2$ in the western Atlantic Ocean, *Paleoceanography*, *20*, PA1017, doi:10.1029/2004PA001021.

Curry, W. B., J. C. Duplessy, L. D. Labeyrie, and N. J. Shackleton (1988), Quaternary deep-water circulation changes in the distribution of $\delta^{13}C$ of deep water ΣCO2 between the last glaciation and the Holocene, *Paleoceanography*, *3*, 317–342, doi:10.1029/PA003i003p00317.

Curry W. B., T. M. Marchitto, J. F. McManus, D. W. Oppo, and K. L. Laarkamp (1999), Millennial-scale changes in ventilation of the thermocline, intermediate and deep waters of the glacial North Atlantic, AGU Chapman Conference volume, *Geophys. Monogr. Ser.*, vol. 112, pp. 59–76.

Dokken, T. M., and E. Jansen (1999), Rapid changes in the mechanism of ocean convection during the last glacial period, *Nature*, *401*, 458–461.

Duplessy, J. C., N. J. Shackleton, R. K. Matthews, W. Prell, W. F. Ruddiman, M. Caralp, and C. H. Hendy (1984), C13 record of benthic foraminifera in the last interglacial ocean: Implications for the carbon cycle and the global deep water circulation, *Quat. Res.*, *21*, 225–243.

Duplessey, J.-C., N. J. Shackleton, R. G. Fairbanks, L. Labeyrie, D. Oppo, and N. Kallel (1988), Deepwater source variations during the last climatic cycle and their impact on the global deep water circulation, *Paleoceanography*, *3*, 343–360, doi:10.1029/PA003i003p00343.

Erez, J., and B. Luz (1983), Experimental paleotemperature equation for planktonic foraminifera, *Geochim. Cosmochim. Acta*, *47*(6), 1025–1031.

Gebbie, G. (2014), How much did Glacial North Atlantic Water shoal?, *Paleoceanography*, *29*, 190–209, doi:10.1002/2013PA002557.

Gherardi, J.-M., L. Labeyrie, S. Nave, R. Francois, J. F. McManus, and E. Cortijo (2009), Glacial-interglacial circulation changes inferred from 231 Pa/230Th sedimentary record in the North Atlantic region, *Paleoceanography*, *24*, PA2204, doi:10.1029/2008PA001696.

Graham, D. W., B. H. Corliss, M. L. Bender, and L. D. Keigwin (1981), Carbon and oxygen isotope disequilibria of Recent deep-sea benthic foraminifera, *Mar. Micropaleontol.*, *6*, 483–497.

Hodell, D. A., J. E. T. Channell, J. Curtis, O. Romero, and U. Röhl (2008), Onset of "Hudson Strait" Heinrich events in the eastern north Atlantic at the end of the middle Pleistocene transition (~640 ka)?, *Paleoceanography*, *23*, PA4218, doi:10.1029/2008PA001591.

Hodell, D. A., H. F. Evans, J. E. T. Channell, and J. H. Curtis (2010), Phase relationships of North Atlantic ice-rafted debris, *Quat. Sci. Rev.*, *29*, 3875–3886.

Hoffman, J. L., and D. C. Lund (2012), Refining the stable isotope budget for Antarctic Bottom Water: New foraminiferal data from the abyssal southwestern Atlantic, *Paleoceanography*, *27*, PA1213, doi:10.1029/2011PA002216.

Huang, K. F., D. W. Oppo, and W. B. Curry (2014), Decreased influence of Antarctic intermediate water in the tropical Atlantic during North Atlantic cold events, *Earth Planet. Sci. Lett.*, *389*, 200–208.

Jouzel, J., et al. (2001), A new 27ky high resolution East Antarctic climate record, *Geophys. Res. Lett.*, *28*, 3199–3202, doi:10.1029/2000GL012243.

Keigwin, L. D. (2004), Radiocarbon and stable isotope constraints on Last Glacial Maximum and Younger Dryas ventilation in the western North Atlantic, *Paleoceanography*, *19*, PA4012, doi:10.1029/2004PA001029.

Keigwin, L. D., and E. A. Boyle (2008), Did North Atlantic overturning halt 17,000 years ago?, *Paleoceanography*, *23*, PA1101, doi:10.1029/2007PA001500.

Keigwin, L. D., and S. J. Lehman (1994), Deep circulation change linked to Heinrich Event-1 and Younger Dryas in a mid-depth North Atlantic core, *Paleoceanography*, *9*, 185–194, doi:10.1029/94PA00032.

Kroopnick, P. (1985), The distribution of 13C and ∑CO2 in the world oceans, *Deep Sea Res., Part A*, *32*, 57–84.

Kwon, E. Y., M. P. Hain, D. M. Sigman, E. D. Galbraith, J. L. Sarmiento, and J. Toggweiler (2012), North Atlantic ventilation of "southern-sourced" deep water in the glacial ocean, *Paleoceanography*, *27*, PA2208, doi:10.1029/2011PA002211.

LeGrand, P., and C. Wunsch (1995), Constraints from paleo-tracer data on the North Atlantic circulation during the last glacial maximum, *Paleoceanography*, *10*, 1011–1045, doi:10.1029/95PA01455.

Liss, P. S., and L. Merlivat (1986), Air-sea gas exchange rates: Introduction and synthesis, in *The Role of Air-Sea Exchange in Geochemical Cycling*, edited by P. Buat-Menard, pp. 113–127, D. Reidel, Norwell, Mass.

Liu, Z., et al. (2009), Transient climate simulation of last deglaciation with a new mechanism for Bølling-Allerød warming, *Science*, *325*, 310–314.

Lund, D. C., A. C. Tessin, J. L. Hoffman, and A. Schmittner (2015), Southwest Atlantic watermass evolution during the last deglaciation, *Paleoceanography*, doi:10.1002/2014PA002657, in press.

Lynch-Stieglitz, J. (2001), Using ocean margin density to constrain ocean circulation and surface wind strength in the past, *Geochem. Geophys. Geosyst.*, *2*, doi:10.1029/2001GC000208.

Lynch-Stieglitz, J., W. B. Curry, and N. Slowey (1999), Weaker Gulf Stream in the Florida Straits during the Last Glacial Maximum, *Nature*, *402*, 644–648.

Lynch-Stieglitz, J., M. W. Schmidt, L. G. Henry, W. B. Curry, L. Skinner, S. Mulitza, R. Zhang, and P. Chang (2014), Muted change in Atlantic Overturning Circulation over some glacial-aged Heinrich Events, *Nat. Geosci.*, *7*, 144–150, doi:10.1038/NGEO2045.

Mackensen, A., H.-W. Hubberten, T. Bickert, G. Fischer, and D. K. Fütterer (1993), The $\delta^{13}C$ of benthic foraminiferal tests of *Fontboita wuellerstorfi* (Schwager) relative to the $\delta^{13}C$ of dissolved inorganic carbon in Southern Ocean deep water: Implications for glacial ocean circulation models, *Paleoceanography*, *8*, 587–610, doi:10.1029/93PA01291.

Makou, M. C., D. W. Oppo, and W. B. Curry (2010), South Atlantic intermediate water mass geometry for the Last Glacial Maximum from foraminiferal Cd/Ca, *Paleoceanography*, *25*, PA4101, doi:10.1029/2010PA001962.

Manabe, S., and R. J. Stouffer (1997), Coupled ocean-atmosphere model response to freshwater input: Comparison to the Younger Dryas event, *Paleoceanography*, *12*, 321–336, doi:10.1029/96PA03932.

Marchal, O., T. F. Stocker, F. Joos, and J. Thiede (1998), A latitude-depth, circulation-biogeochemical ocean model for paleoclimate studies. Development and sensitivities, *Tellus*, *50B*, 290–316.

Marchitto, T. M., and W. S. Broecker (2006), Deep water mass geometry in the glacial Atlantic Ocean: A review of constraints from the paleonutrient proxy Cd/Ca, *Geochem. Geophys. Geosyst.*, *7*, Q12003, doi:10.1029/2006GC001323.

Marchitto, T. M. J., Oppo, D. W., and Curry, W. B. (2002), Paired benthic foraminiferal Cd/Ca and Zn/Ca evidence for a greatly increased presence of Southern Ocean Water in the glacial North Atlantic, *Paleoceanography*, *17*(3), 1038, doi:10.1029/2000PA000598.

Marcott, S. A., et al. (2011), Ice-shelf collapse from subsurface warming as a trigger for Heinrich events, *Proc. Natl. Acad. Sci. U.S.A.*, *108*, 13,415–13,419.

McManus, J. F., R. Francois, J. Gherardi, L. D. Keigwin, and S. Brown-Leger (2004), Large and rapid deglacial changes in Atlantic meridional circulation recorded in sedimentary Pa/Th, *Nature*, *424*, 834–837.

Meckler, A. N., D. M. Sigman, K. A. Gibson, R. François, A. Martínez-García, S. L. Jaccard, U. Rohl, L. C. Peterson, R. Tiedemann, and G. H. Haug (2013), Deglacial pulses of deep-ocean silicate into the subtropical North Atlantic Ocean, *Nature*, *495*(7442), 495–498.

Meland, M. Y., T. M. Dokken, E. Jansen, and K. Hevroy (2008), Water mass properties and exchange between the Nordic seas and the northern North Atlantic during the period 23–6 ka: Benthic oxygen isotopic evidence, *Paleoceanography*, *23*, PA1210, doi:10.1029/2007PA001416.

Mix, A. C., and R. G. Fairbanks (1985), North Atlantic surface-ocean control of Pleistocene deep-ocean circulation, *Earth Planet. Sci. Lett.*, *73*, 231–243.

Mook, W. G., J. C. Bommerson, and W. H. Staverman (1974), Carbon isotope fractionations between dissolved bicarbonate and gaseous carbon dioxide, *Earth Planet. Sci. Lett.*, *22*, 169–176.

Oppo, D. W., and W. B. Curry (2012), Deep Atlantic circulation during the Last Glacial Maximum and deglaciation, *Nat. Educ. Knowl.*, *3*(4).

Oppo, D. W., and R. G. Fairbanks (1987), Variability in the deep and intermediate water circulation of the Atlantic Ocean: Northern Hemisphere modulation of the southern ocean, *Earth Planet. Sci. Lett.*, *86*, 1–15.

Oppo, D. W., and S. J. Lehman (1993), Mid-depth circulation of the subpolar North Atlantic during the Last Glacial Maximum, *Science*, *259*, 1148–1152.
Pahnke, K., S. L. Goldstein, and S. R. Hemming (2008), Abrupt changes in Antarctic Intermediate Water circulation over the past 25,000 years, *Nat. Geosci.*, *1*, 870–874.
Praetorius, S. K., J. F. McManus, D. W. Oppo, and W. B. Curry (2008), Episodic reductions in bottom-water currents since the last ice age, *Nat. Geosci.*, *1*, 449–452.
Reimer, P. J., et al. (2013), INTCAL13 and MARINE13 Radiocarbon age calibration curves 0–50,000 Years CAL BP, *Radiocarbon*, *55*, 1869–1887.
Rickaby, R. E. M., and H. Elderfield (2005), Evidence from the high-latitude North Atlantic for variations in Antarctic Intermediate Water flow during the last deglaciation, *Geochem. Geophys. Geosyst.*, *6*, Q05001 doi:10.1029/2004GC000858.
Roberts, N. L., A. Piotrowski, J. F. McManus, and L. D. Keigwin (2010), Synchronous deglacial overturning and source watermass changes, *Science*, *327*, 75–78.
Robinson, L. F., J. F. Adkins, L. D. Keigwin, J. Southon, D. P. Fernandez, S. L. Wang, and D. S. Scheirer (2005), Radiocarbon variability in the Western North Atlantic during the last deglaciation, *Science*, *310*, 1469–1473.
Rühlemann, C., S. Mulitza, G. Lohmann, A. Paul, M. Prange, and G. Wefer (2004), Intermediate depth warming in the tropical Atlantic related to weakened thermohaline circulation: Combining paleoclimate data and modeling results for the last deglaciation, *Paleoceanography*, *19*, PA1025, doi:10.1029/2003PA000948.
Schmidt, M. W., P. Chang, J. E. Hertzberg, T. R. Them, L. Ji, and B. L. Otto-Bliesner (2012), Impact of abrupt deglacial climate change on tropical Atlantic subsurface temperatures, *Proc. Natl. Acad. Sci. U.S.A.*, *109*, 14,348–14,352.
Schmitt, J., et al. (2012), Carbon isotope constraints on the deglacial $CO_2$ rise from ice cores, *Science*, *336*, 711–714.
Schmittner, A., and D. C. Lund (2015), Early deglacial Atlantic overturning and its role for atmospheric $CO_2$ rise as inferred from carbon isotopes ($\delta^{13}C$), *Clim. Past*, *11*, 135–152.
Sigman, D. M., A. M. de Boer, and G. H. Haug (2008), Antarctic stratification, atmospheric water vapor, and Heinrich events: A hypothesis for late Pleistocene deglaciations, in *Past and Future Changes of the Oceanic Meridional Overturning Circulation: Mechanisms and Impacts*, *Geophys. Monogr. Ser.*, vol. 173, edited by A. Schmittner, J. H. Chiang, and S. R. Hemming, pp. 335–350, AGU, Washington, D. C.
Sigman, D. M., M. P. Hain, and G. H. Haug (2010), The polar ocean and glacial cycles in atmospheric CO2 concentration, *Nature*, *466*, 47–55.
Skinner, L. C., and N. J. Shackleton (2004), Rapid transient changes in northeast Atlantic deep water ventilation age across Termination I, *Paleoceanography*, *19*, PA2005, doi:10.1029/2003PA000983.
Stern, J. V., and L. E. Lisiecki (2013), North Atlantic circulation and reservoir age changes over the past 41,000 years, *Geophys. Res. Lett.*, *40*, 3693–3697, doi:10.1002/grl.50679.
Stuiver, M., P. D. Quay, and H. G. Ostlund (1983), Abyssal water carbon-14 distributions and the age of the world oceans, *Science*, *219*, 849–851.
Tessin, A., and D. C. Lund (2013), Isotopically depleted carbon in the mid-depth South Atlantic during the last deglaciation, *Paleoceanography*, *28*, 296–306, doi:10.1002/palo.20026.
Thornalley, D. J. R., H. Elderfield, and I. N. McCave (2010), Intermediate and Deep Water Paleoceanography of the northern North Atlantic over the last 21,000 years. *Paleoceanography*, *25*, PA1211, doi:10.1029/2009PA001833.
Thornalley, D. J. R., S. Barker, W. S. Broecker, H. Elderfield, and I. N. McCave (2011), The deglacial evolution of North Atlantic deep convection, *Science*, *331*, 202–205.
Toggweiler, J. R., J. L. Russell, and S. R. Carson (2006), Midlatitude westerlies, atmospheric $CO_2$, and climate change during the ice ages, *Paleoceanography*, *21*, PA2005, doi:10.1029/2005PA001154.
Vidal, L., L. Labeyrie, E. Cortijo, M. Arnold, J. C. Duplessy, E. Michel, S. Becque, and T. C. E. van Weering (1997), Evidence for changes in the North Atlantic Deep Water linked to meltwater surges during the Heinrich events, *Earth Planet. Sci. Lett.*, *146*, 13–27.
Vidal, L., L. Labeyrie, and T. C. E. van Weering (1998), Benthic $\delta^{18}O$ records in the North Atlantic over the last glacial period (60–10kyr): Evidence for brine formation, *Paleoceanography*, *13*, 245–251, doi:10.1029/98PA00315.
Waelbroeck, C., C. Levi, J. C. Duplessy, L. Labeyrie, E. Michel, E. Cortijo, F. Bassinot, and F. Guichard (2006), Distant origin of circulation changes in the Indian Ocean during the last deglaciation, *Earth Planet. Sci. Lett.*, *243*, 244–251.
Waelbroeck, C., L. Skinner, L. Labeyrie, J.-C. Duplessy, E. Michel, N. V. Riveiros, J.-M. Gherardi, and F. Dewilde (2011), The timing of deglacial circulation changes in the Atlantic, *Paleoceanography*, *26*, PA3213, doi:10.1029/2010PA002007.
Wunsch, C. (2003), Determining paleoceanographic circulations with emphasis on the Last Glacial Maximum, *Quat. Sci. Rev.*, *22*, 371–385.
Xie, R. C., F. Marcantonio, and M. W. Schmidt (2012), Deglacial variability of Antarctic Intermediate Water penetration into the North Atlantic from authigenic neodymium isotope ratios, *Paleoceanography*, *27*, PA3221, doi:10.1029/2012PA002337.
Yu, J., W. S. Broecker, H. Elderfield, Z. Jin, J. McManus, and F. Zhang (2010), Loss of carbon from the deep sea since the Last Glacial Maximum, *Science*, *330*, 1084–1087.
Yu, J., R. F. Anderson, Z. Jin, L. Menviel, F. Zhang, F. J. Ryerson, and E. J. Rohling (2014), Deep South Atlantic carbonate chemistry and increased interocean deep water exchange during last deglaciation, *Quat. Sci. Rev.*, *90*, 80–89.
Zahn, R., and A. Stuber (2002), Suborbital intermediate water variability inferred from paired benthic foraminiferal Cd/Ca and delta C-13 in the tropical West Atlantic and linking with North Atlantic climates, *Earth Planet. Sci. Lett.*, *200*, 191–205.